Supporting information

Sustainable earth-abundant bismuth catalytic nanointerfaces using biopolymeric silk fibroin for efficient pollutant reduction

Md. Hasan Ali[1], Md. Abdur Rahman[1*], Anwar Ul Hamid[2], Hasan Ahmad[1]
[1]*Polymer Colloids and Nanomaterisearch Lab, Department of Chemistry, Faculty of Science, University of Rajshahi, Rajshahi-6205, Bangladesh*
[2]*Core Research Facilities, King Fahd University of Petroleum and Minerals, 31261 Dhahran, Saudi Arabia*
[*]Correspondence: arahman@ru.ac.bd, ORCID: 0000-0002-3855-8160

The supporting Information includes:

Supplementary Table S1.

Supplementary Fig. S1 to S5.

Table S1: Recipe for the extraction of biopolymeric SF from the *Bombyx mori* Rajshahi silk.

Ingredients	Amount (g)	Yield (%)
Silk cocoons	12.4397	72
Na_2CO_3	0.954	
H_2O	100	

Conditions: 0.02 M Na_2CO_3, 500 rpm, 2 h, 100 °C.

Typical energy-dispersive X-ray spectroscopy (EDS) performed at 20 keV confirms the elemental distribution of bare-Bi and Bi/SF nanointerfaces (2:1) shown in Fig. S1. The bare-Bi sample (a) exhibits a dominant Bi signal (81.76 at%), accompanied by minor contributions from oxygen (11.65 at%), carbon (4.65 at%), and nitrogen (1.95 at%). This profile reflects surface passiation with oxalates which is common in glycolic solvothermal method, oxidation, adventitious carbon and nitro-precursors of typical of metallic-Bi systems. In contrast, the Bi/SF nanohybrid (b) shows a reduced Bi content (72.17 at%) with a marked increase in carbon (17.14 at%), consistent with the incorporation of SF. Oxygen (9.09 at%) and nitrogen (1.60 at%) remain present, further supporting the biopolymeric contribution. The compositional shift highlights the successful integration of SF as a stabilizing matrix, which both lowers the relative Bi signal and enhances the organic signature.

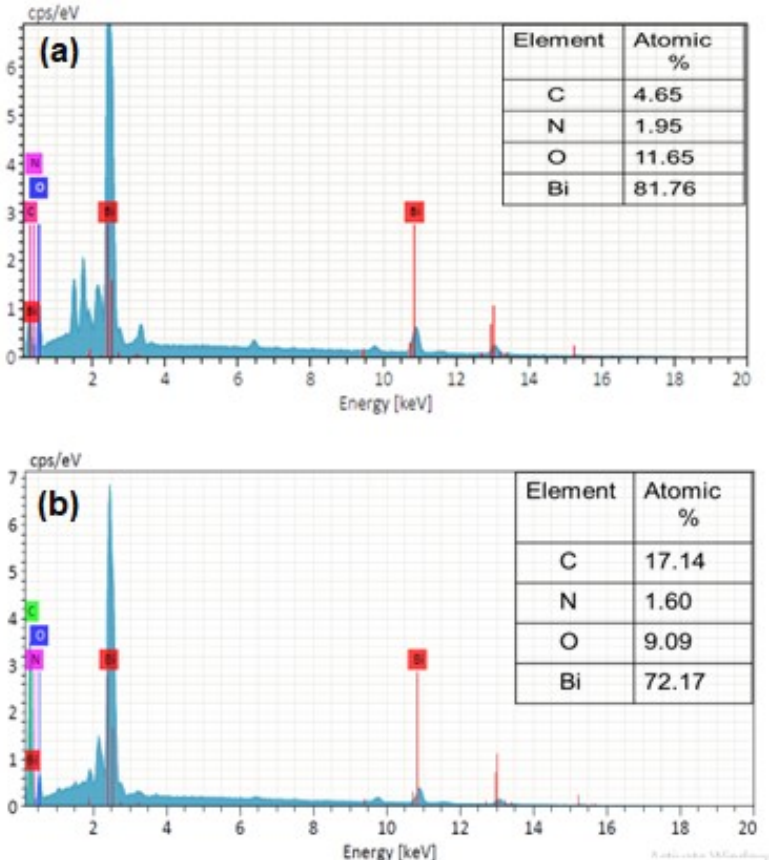

Fig. S1. Typical EDX spectra and atom% of bare-Bi (a), and (b) Bi/SF (2:1) measured at 20 keV.

Fig. S2 reveals distinct size distributions for bare-Bi and Bi/SF nanointerfaces prepared by varying Bi:SF ratios. Bare-Bi (Fig. S2a) exhibits a broad distribution with an average hydrodynamic diameter (D_h) of 233 nm (CV = 0.523, SD = 122 nm), indicative of significant polydispersity and aggregation tendencies due to absence of any polymeric stabilizer. Upon incorporation of SF, the particle size distributions shift markedly toward smaller and more uniform populations. At a Bi:SF ratio of 2:1, the D_h came to 134 nm (CV = 0.479, SD = 64 nm), while ratios of 4:1 and 6:1 yielded average diameters of 144 nm (CV = 0.461, SD = 66 nm), and 162 nm (CV = 0.502, SD = 81 nm), respectively (Fig. S2bcd). These results highlight the stabilizing role of the SF-biopolymeric matrix, which reduced aggregation and enhances colloidal uniformity.[S1]

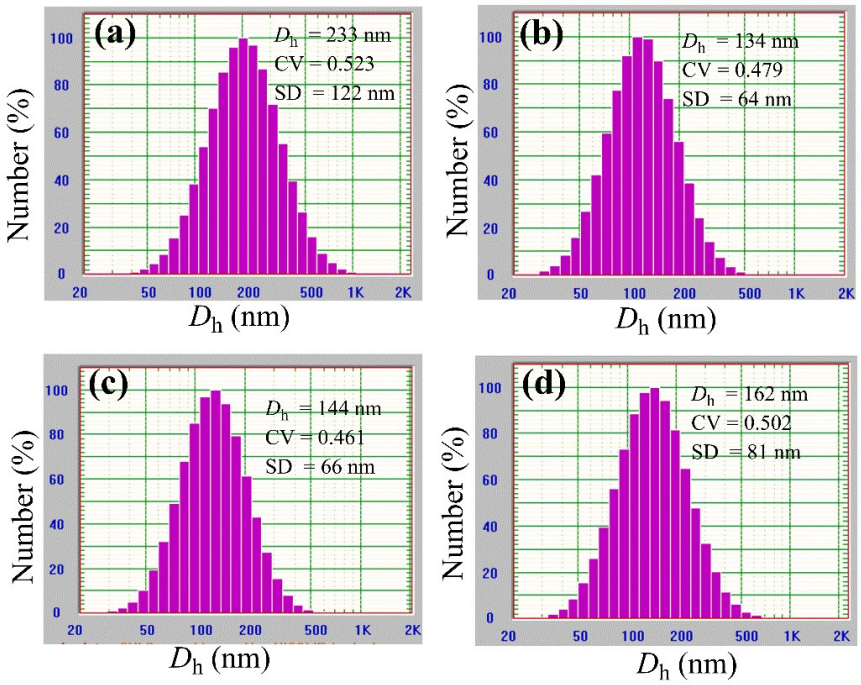

Fig. S2. Typical DLS profiles for D_h of bare-Bi (a) and Bi/SF interfaces having the Bi to SF ratios of (b) 2:1, (c) 4:1 and (d) 6:1 measured by dynamic light scattering methods in aqueous buffer at 25 °C.

Fig. S3 shows the time-resolved UV-vis spectra (190-690 nm) reveals the efficient catalytic reduction of Eriochrome Black T (EBT) in aqueous medium by Bi/SF nanointerfaces under mild conditions (25 °C, EBT 34 mg L^{-1}, $NaBH_4$ 0.5 mg, catalyst 0.2 mg, total volume 50 mL). The characteristic absorption band at 530 nm, corresponding to the azo chromophore, remains unchanged in the presence of $NaBH_4$ alone, confirming its limited reducing ability. In contrast, the Bi/SF system induces a rapid decline in absorbance intensity, with near-complete disappearance of the 530 nm band within 2 minutes, consistent with azo bond cleavage and dye reduction.

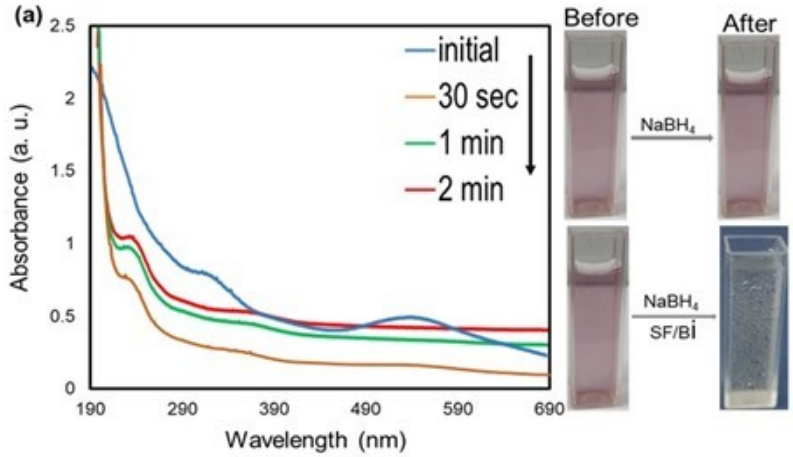

Fig. S3: (a) Time-dependent UV-vis spectra for catalytic reduction of EBT. Conditions: Temperature: 25 °c, EBT: 35 mg/L, $NaBH_4$: 0.5 mg, Catalyst: 0.2 mg, Total volume: 50 mL.

Fig. S4a exhibits the reduction of CR exhibited the fastest kinetics with a slope of -0.316, and regression constant (R^2 was 0.997), indicating rapid azo bond cleavage and highly consistent data fitting. While for MO, the reduction kinetics followed with a slope of -0.139 and an R^2 of 0.993, reflecting relatively slower azo reduction due to lower adsorption affinity and electron demand (Fig. S4b). In the reduction of *p*-NA showed intermediate kinetics (slope, 0.231, R^2 0.984), consistent with nitro-to-amine conversion requiring multi-electron transfer steps (Fig. S4c). In contrast, EBT, a complex azo compound having sulfonates and hydroxyl groups, displayed a slope of -0.251, and R^2 of 0.966, revealed moderately faster reduction (Fig. S4d). However, it showed slightly more variability than other substrates, likely due to steric hindrance and weaker dye-SF interactions. Overall, the kinetic order was CR>EBT≈p-NA>MO, with all reactions showing strong linearity and reproducibility. These results confirm that Bi/SF nanointerfaces facilitate efficient electron relay and substrate-specific adsorption, enabling rapid and selective reduction under mild conditions.

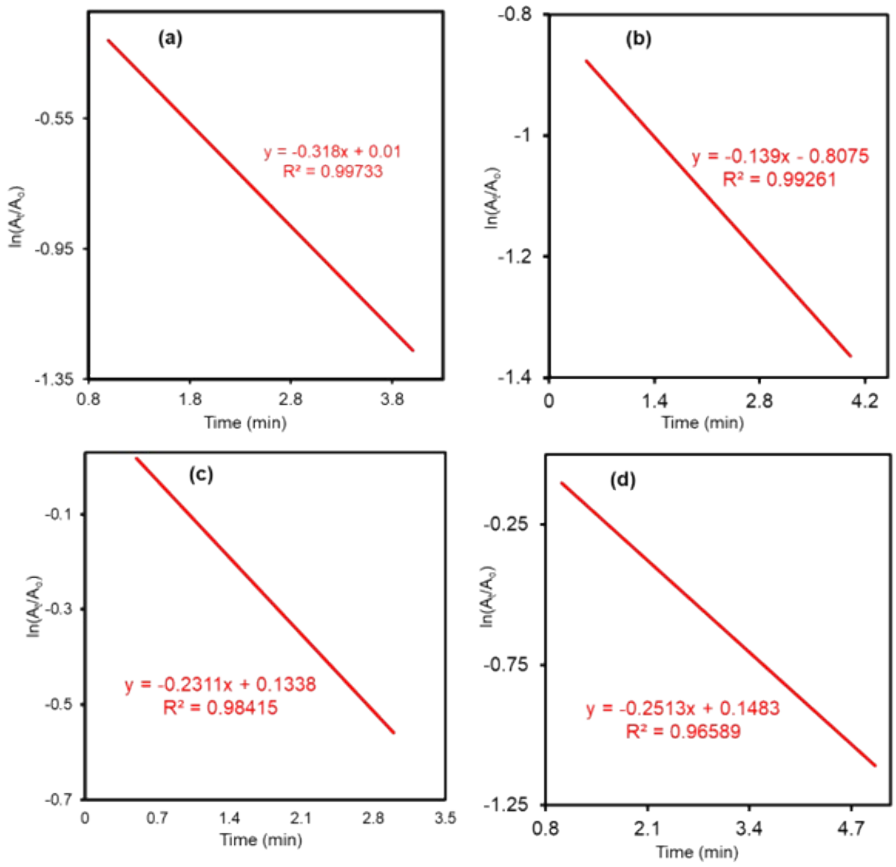

Fig. S4: Kinetic modeling for reducing CR, MO, EBT and *p*-NA using Bi/SF nanointerfaces in aqueous $NaBH_4$ at ambient conditions.

The stability and structural integrity of Bi/SF (2:1) nanointerfaces was confirmed by FTIR and PXRD analyses after using five catalytic cycles in reducing azo and nitro pollutants. The FTIR spectrum (Fig.S5a) displays a broad band at 3500-32500 cm^{-1} corresponding to O-H and N-H stretching vibrations. Likewise, the weak signals appear at 2920 cm^{-1} and 3070 cm^{-1} for aliphatic and aromatic C-H stretching. The sharp band near 1667 cm^{-1} is attributed to C=O stretching, while the buried peaks at 1448-1320 cm^{-1} corresponds to aromatic C=C stretching. O-H/N-H bending bands appeared at 1540 cm^{-1} and C-O stretching was seen at 1077 cm^{-1}) further confirm the persistence of SF. Importantly, the strong band at 560 cm^{-1} assignable to Bi-O stretching, remains prominent after repeated use, which is demonstrating the stability of the Bi-oxide network on the surface of metallic-Bi phase under redox conditions.

PXRD analysis (Fig. S5b) reveals sharp reflections centered for the (003), (012), (015), (104), (110), (006), (202), (024), (116), (122), (214), and (125) planes, almost consistent with metallic-Bi (JCPDS # 01-085-1330). The absence of others impurity peaks indicates phase

purity and confirms that SF-matrix does not allow to introduce crystalline contaminants via ligating products yielded from reduction reactions. The persisting Bi-reflections after multiple cycles highlights the robustness of metallic-Bi domains, ensuring reproducible electron transfer pathways during pollutant reductions. Both FTIR and PXRD results demonstrate that the hybrid Bi/SF (2:1) nanointerfaces retain both organic and inorganic features after repeated catalytic usage. This dual stability underscores their potential as sustainable catalytic platforms for pollutants remediation.

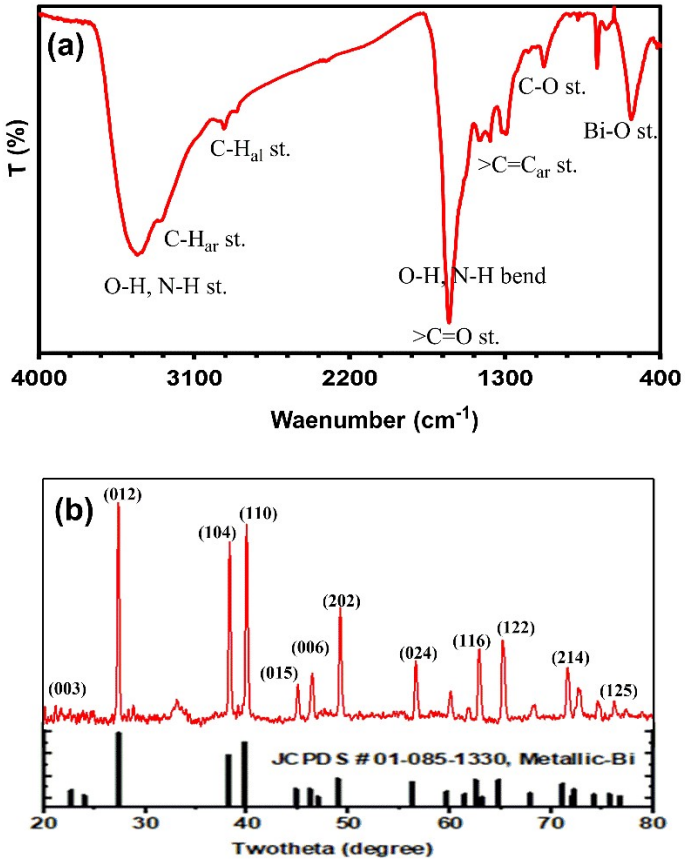

Fig. S5: Stability of recycled Bi/SF (2:1) nanointerfaces using (a) FTIR and (b) PXRD analyses.

Supporting references:

S1. X Gu, Y Yu, S Zhong, Y Zhang, H Liu, J Wang, Q Li, R Chen, Y Zhao and Y Liu, *Adv. Fiber Mater.*, **2025**, *7*, 1529–1544.

S2. Y Zhang, Y Huang, L Chen and Y Zhao, *ACS Sustainable Chem. Eng.*, **2023**, *11*, 3456–3465.